

## LQCD: Flavor Physics and Spectroscopy

---

**Carleton DeTar\***

*Department of Physics and Astronomy, University of Utah, Utah 84112, USA*

*E-mail:* [detar@physics.utah.edu](mailto:detar@physics.utah.edu)

I review highlights of recent results in quark-flavor physics and heavy-quark spectroscopy from lattice QCD, with emphasis on  $B$ -meson decays and excited and exotic charmonium states.

*International Symposium on Lepton Photon Interactions at High Energies*

*17-22 August 2015*

*University of Ljubljana, Slovenia*

---

\*Speaker.

## 1. Introduction

The numerical simulation of lattice quantum chromodynamics (QCD) has made enormous strides over the past two decades thanks to advances in computing power and algorithms. It is now the method of choice for studying QCD in the static, nonperturbative regime, *e.g.* for such properties as hadronic structure, spectroscopy, and transition amplitudes and for studying hot and dense QCD in thermal equilibrium. The lattice serves as an ultraviolet regulator, and, with suitable renormalization and the continuum limit, it is expected to fall in the same universality class as QCD with any of the popular continuum regulators. Thus lattice QCD is an *ab-initio* method in that its results can be refined to arbitrary precision (given enough computing power). There are no uncontrolled model approximations.

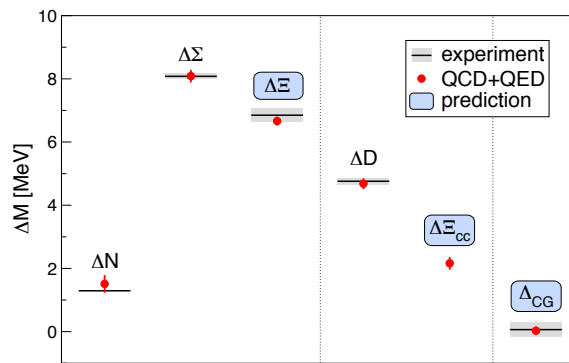


**Figure 1:** Charge-multiplet mass splittings of the  $\frac{1}{2}^+$  baryon octet from a lattice QED+QCD calculation compared with the experimental values [1]. Such calculations are excellent tests of the lattice methodology.

We validate our numerical methodology by comparing results of calculations with well-established measurements. An impressive recent example is the Budapest-Marseille-Wuppertal calculation of the electromagnetic splittings of the baryon octet, shown in Fig. 1 [1]. This lattice calculation included both QCD and quantum electrodynamics.

A variety of lattice formulations of QCD are in wide current use. They differ particularly in their fermion formulation. Each has its good and bad points. However, all are expected to result in the same theory in the continuum limit. Thus it is useful to carry out important calculations with more than one lattice formulation as a cross check. For quark-flavor physics, the Flavor Lattice Averaging Group provides biennial reviews of recent lattice results drawing from the wide variety of lattice formulations [2]. A new review is expected later in 2015.

In assessing the quality of the result of a lattice calculation, one should look for the following features: (1) Was the calculation done at multiple lattice spacings and has the continuum limit been taken? (2) Was the lattice volume large enough that finite volume effects are under control? (3) What sea quark flavors have been included? Many studies now include charm sea quarks as well as strange, up, and down, but some still include only up and down. (4) Were all quark masses at their physical values? If not, was a suitable extrapolation/interpolation carried out to reach the physical masses? (5) Was a complete analysis of systematic errors undertaken?

To be sure, lattice QCD has its limitations. It is not well suited to the study of real-time behavior. Phenomena such as the evolution of hadronic jets and multiparticle scattering are not

easily treated. At high temperature, only thermodynamic equilibrium and perturbations thereof, including transport properties, are feasible [3]. Out-of-equilibrium processes are very difficult subjects.

My task in this brief talk is to review recent lattice-QCD highlights in quark-flavor physics and in spectroscopy. For quark-flavor physics, I will focus on  $B$ -meson decays and tests of the standard model. For spectroscopy, I will describe progress in studies of excited and exotic charmonium states.

## 2. Quark-flavor-physics highlights

The experimental and theoretical flavor-physics programs aim to obtain accurate values of standard-model parameters and especially to subject the standard model to stringent tests in the hope of discovering evidence for new physics. High-precision tests extend the high-energy reach of experiment. Tree-level leptonic and semileptonic decays of heavy mesons to light charged leptons are thought to provide reliable determinations of standard-model parameters free of significant new-physics contamination. Rare decays of heavy mesons involving higher-order electroweak processes are hoped to be a particularly promising place to find evidence for physics beyond the standard model. The same is true of neutral-meson mixing, which is intrinsically higher order. Although these processes arise from electroweak interactions, any process involving hadrons necessarily also involves QCD, so lattice QCD is needed in order to simulate the decay environment and expose the underlying electroweak physics.

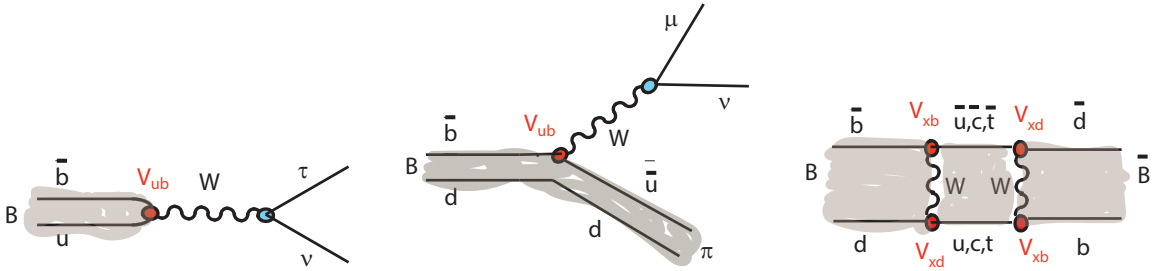


**Figure 2:** Typical valence quark-line diagrams for  $B$ -meson processes: (left) leptonic decay, (middle) semileptonic decay, and (right) one of the neutral  $B$ -meson mixing diagrams. The shaded regions denote strong interactions.

The Cabibbo-Kobayashi-Maskawa (CKM) matrix parameterizes the mixing between quark flavors under charged weak interactions. In the standard model it is unitary. Thus a popular test checks unitarity. CKM matrix elements are typically determined from flavor transitions in leptonic or semileptonic decays or in neutral meson mixing. Some relevant valence quark-line diagrams are shown in Fig. 2. The underlying electroweak processes are treated in perturbation theory, but the strong interactions are treated nonperturbatively in lattice gauge theory. So, for example, the standard model  $B \rightarrow \pi \ell \nu$  differential decay rate

$$d\Gamma/dq^2 \propto |V_{ub}|^2 |f_+(q^2)|^2, \quad (2.1)$$

depends on the CKM matrix element  $|V_{ub}|$  and the nonperturbative hadronic form factor  $|f_+(q^2)|$ , which is computed in lattice QCD. The proportionality constant is a product of a known kinematic

factor and the squared Fermi constant. So we can solve for  $|V_{ub}|$  and use the result in the test of CKM unitarity. The error in the result is a combination of experimental and theoretical errors. Clearly, to make progress in precision, it is important that both errors be reduced in parallel.

Similar considerations apply for leptonic decays and neutral meson mixing. Recent summaries of results for CKM matrix elements may be found in Refs. [2, 4, 5, 6, 7, 8].

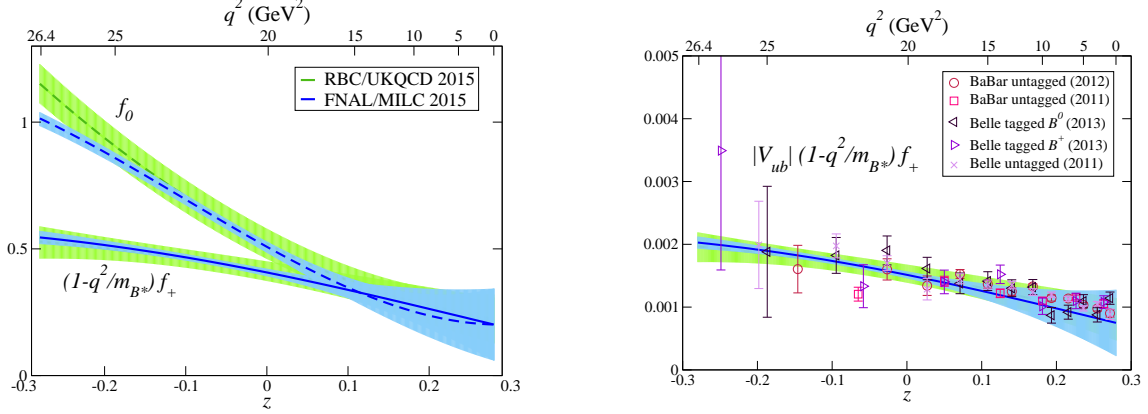


**Figure 3:** Left panel: a comparison of lattice results for the  $B \rightarrow \pi$  vector ( $f_+$ ) and scalar ( $f_0$ ) form factors from the RBC/UKQCD collaboration (green band) [12] and from the Fermilab/MILC collaboration (blue band) [13]. The lattice methods are different but the agreement is excellent. Right panel: a comparison of the theoretical form factors  $f_+$  in the left plot with the experimental differential decay rate. The measured shape is nicely reproduced. (Figure credit [7]).

## 2.1 $B \rightarrow \pi \ell \nu$ at nonzero recoil

In this talk, I highlight mostly results involving  $B$  physics for which several new results were reported in the past few months. A principal challenge for  $B$  physics is gaining control of the lattice discretization errors. This is achieved either through the Fermilab approach [9] or the RHQ variant thereof [10], a nonrelativistic treatment [11], or working with lattice spacings  $a < 1/m_b \approx 0.05$  fm (for  $b$ -quark mass  $m_b$ ), followed by a careful extrapolation to zero lattice spacing. This has been done in two new studies of the semileptonic decay  $B \rightarrow \pi \ell \nu$ . Results for the form factors from two different lattice methods are plotted in Fig. 3. The RBC/UKQCD calculation [12] is based on ensembles generated with domain-wall quarks and uses the RHQ action for the  $b$  quark. The Fermilab Lattice/MILC calculation [13] is based on ensembles generated with the asqtad action with clover  $b$  quarks in the Fermilab interpretation. It yields an error of approximately 3.5% in the vector form factor  $f_+$  in the central kinematic range. The results are extended over the whole kinematic range using a model-independent “ $z$ ” expansion based on the known analytic structure of the form factor. Using this expansion and fitting the Fermilab/MILC form factors with a combination of recent Babar [14, 15] and Belle [16, 17] data then results in the value  $|V_{ub}| = 3.72(16) \times 10^{-3}$ .

## 2.2 $B \rightarrow D \ell \nu$ at nonzero recoil

A determination of  $|V_{cb}|$  from the semileptonic decay  $B \rightarrow D \ell \nu$  rate is best done at nonzero recoil where the relative experimental and theoretical uncertainties are small. In the past year, results from two new lattice calculations at nonzero recoil were reported [18, 19]. These were the

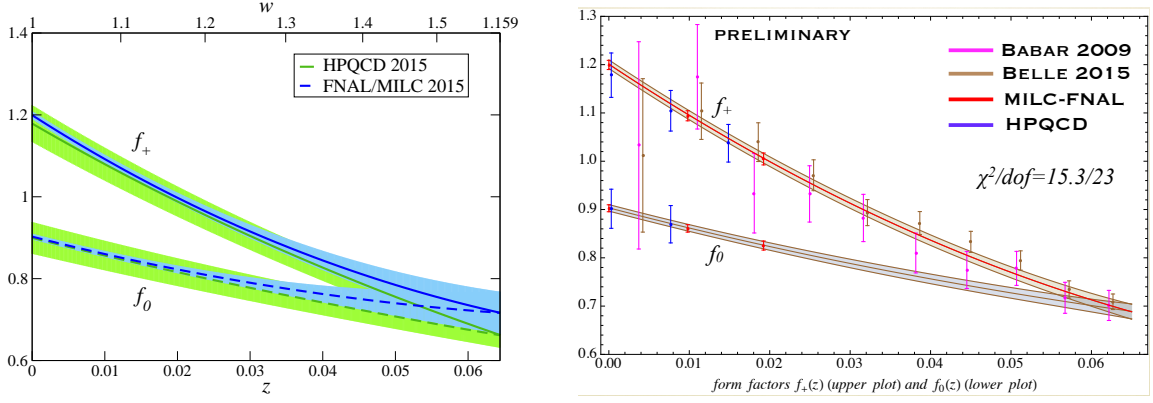


**Figure 4:** Left: Vector and scalar form factors for  $B \rightarrow D\ell\nu$  from two recent lattice calculations [18, 19]. The agreement is good. (Figure credit: [5]). Right: Joint fit of the form factors on the left and experimental data from BaBar [20] and preliminary data from Belle [21, 22]. (Figure credit: [22]).

first such calculations to take into account the effects of sea quarks. Both groups used gauge-field ensembles created by the MILC collaboration based on 2+1 flavors of asqtad sea quarks, resulting in some overlap of inputs. However, the treatments were otherwise independent. Results for both the vector and scalar form factors are shown in the left panel of Fig. 4. The agreement is very good. A combined fit including both new theoretical results and recent Babar [20] and Belle [21, 22] data is shown in the right panel, and yields the value  $|V_{cb}| = 40.7(1.0)_{\text{latQCD}+\text{expt}}(0.2)_{\text{QED}} \times 10^{-3}$ .

### 2.3 $R(D)$

Semileptonic decays of the  $B$  meson,  $B \rightarrow D\ell\nu$  and  $B \rightarrow D^*\ell\nu$  can result in a  $\tau$  lepton as well as  $e$  or  $\mu$ . The quantities  $R(D)$  and  $R(D^*)$  are ratios of branching ratios for decays producing a  $\tau$  or a  $\mu$ :

$$R(D^{(*)}) = \frac{\Gamma(B \rightarrow D^{(*)}\tau\nu)}{\Gamma(B \rightarrow D^{(*)}\mu\nu)}, \quad (2.2)$$

and are studied as a test for new physics. In 2012 the BaBar collaboration reported a value  $R(D) = 0.440(58)(42)$  and  $R(D^*) = 0.332(24)(18)$  [23], which created some excitement because it disagreed with a standard model expectation:  $R(D) = 0.297(17)$  and  $R(D^*) = 0.252(3)$  [24] at the  $3.5\sigma$  level. This year's new experimental results from the Belle and LHCb collaborations,  $R(D) = 0.375(64)(26)$  and  $R(D^*) = 0.293(38)(15)$  [26] and  $R(D^*) = 0.366(27)(30)$  [27], confirm the discrepancy with the standard model; the HFAG combination of all measurements disagrees at  $3.9\sigma$  [28].

### 2.4 Exclusive vs. inclusive $|V_{cb}|$ and $|V_{ub}|$ .

There has been a long-standing tension between determinations of  $|V_{cb}|$  and  $|V_{ub}|$  from inclusive and exclusive  $B$ -meson decays. Figure 5 illustrates the severity of this tension by plotting results from (1) the four recent exclusive semileptonic decays described above; (2) a recent calculation of  $B \rightarrow D^*\ell\nu$  [29]; and (3) the result for the ratio  $|V_{cb}|/|V_{ub}|$  from a recent calculation of the exclusive semileptonic decay ratios  $\Gamma(\Lambda_b \rightarrow p\ell\nu)/\Gamma(\Lambda_b \rightarrow \Lambda_c\ell\nu)$  by Detmold, Lehner, and Meinel [30]. The result of a simple weighted average of all six lattice calculations

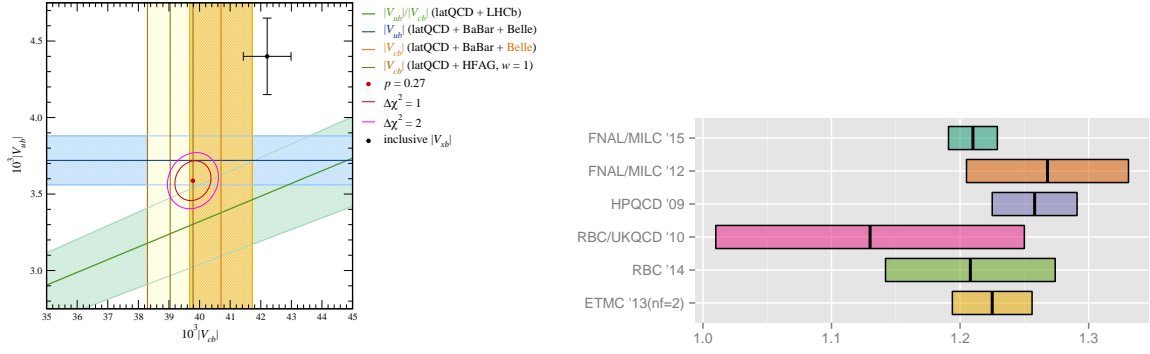


**Figure 5:** Left: determination of  $|V_{cb}|$  and  $|V_{ub}|$  using a fit to recent lattice results for the exclusive processes  $B \rightarrow \pi \ell \nu$  [12, 13] (blue band),  $B \rightarrow D^* \ell \nu$  [29] (light yellow band),  $B \rightarrow D \ell \nu$  [18, 19] (dark yellow band) and the ratio of differential decay rates  $\Gamma(\Lambda_b \rightarrow p \ell \nu) / \Gamma(\Lambda_b \rightarrow \Lambda_c \ell \nu)$  [30] (pale green diagonal band). The exclusive determinations are compatible at the  $p = 0.27$  level. The inclusive determinations [28, 31], shown by the cross, display a strong tension with the  $1\sigma$  and  $2\sigma$  error ellipses. (Figure credit: [32]). Right: comparison of a recent preliminary result for the  $B$ -mixing ratio  $\xi$  from Ref. [38] with previous results [33, 34, 35, 36, 37].

gives  $|V_{cb}| = 39.78(42) \times 10^{-3}$  and  $|V_{ub}| = 3.59(9) \times 10^{-3}$ . The nonlattice inclusive values from Refs. [31, 28] plotted there differ by several standard deviations.

## 2.5 Neutral $B$ -meson mixing

Mixing in the  $B_x^0$  ( $x = d, s$ ) system occurs at second order in the electroweak interaction; it is parameterized by, among other terms, the CKM matrix element  $|V_{tx}|$  and the hadronic expectation value  $\langle O_{1x} \rangle$  of a  $\Delta B = 2$  four-quark operator  $O_{1x}$ . The mixing strength can be parameterized by the experimentally measured mass splitting  $\Delta M_B$ . It is popular to consider the ratio  $\xi$  of mixing strengths for  $B^0$  and  $B_s^0$  for which many theoretical uncertainties cancel

$$\xi = \frac{M_{B^0}}{M_{B_s^0}} \sqrt{\frac{\langle O_{1s} \rangle}{\langle O_{1d} \rangle}} = \left| \frac{V_{td}}{V_{ts}} \right| \sqrt{\frac{\Delta M_{B_s^0} M_{B^0}}{\Delta M_{B^0} M_{B_s^0}}}. \quad (2.3)$$

Thus the combination of theory and experiment yields the ratio of CKM matrix elements  $|V_{td}/V_{ts}|$ .

In the past year, a new lattice calculation [38] has produced a preliminary value  $\xi = 1.210(19)$ , which is compared with recent results in Fig. 5. It yields a new, preliminary value  $|V_{td}/V_{ts}| = 0.2069(6)_{\text{exp}}(32)_{\text{thy}}$ . Here experiment is still quite a bit ahead of theory in precision.

The “unitarity triangle” provides a graphical illustration of the orthogonality of two rows of the CKM matrix as expected from unitarity. In Fig. 6 we show the effect on the unitarity triangle of recent results from exclusive semileptonic decays for  $|V_{cb}|$  and  $|V_{ub}|$  and the preliminary result for  $|V_{td}/V_{ts}|$  discussed above. So far the result is compatible with three-generation CKM unitarity.

## 2.6 Flavor-changing neutral currents

The processes  $B \rightarrow \pi \ell \ell$  and  $B \rightarrow K \ell \ell$  occur at second-order in the electroweak interaction and are sensitive to new flavor-changing-neutral-current processes. Recent lattice calculations have produced improved differential decay rates [13, 44, 47]. See also Ref. [45]. They are compared

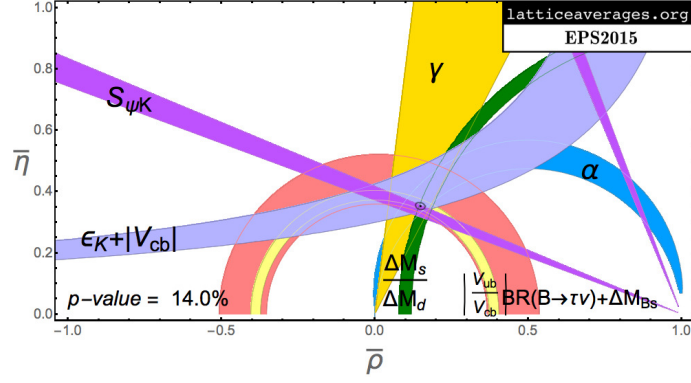


**Figure 6:** Unitarity triangle fit using the new average  $|V_{ub}|$  and  $|V_{cb}|$  exclusive values from Fig. 5 and the new, preliminary value of  $\xi$  from Ref. [38]. (Figure credit: [39]).

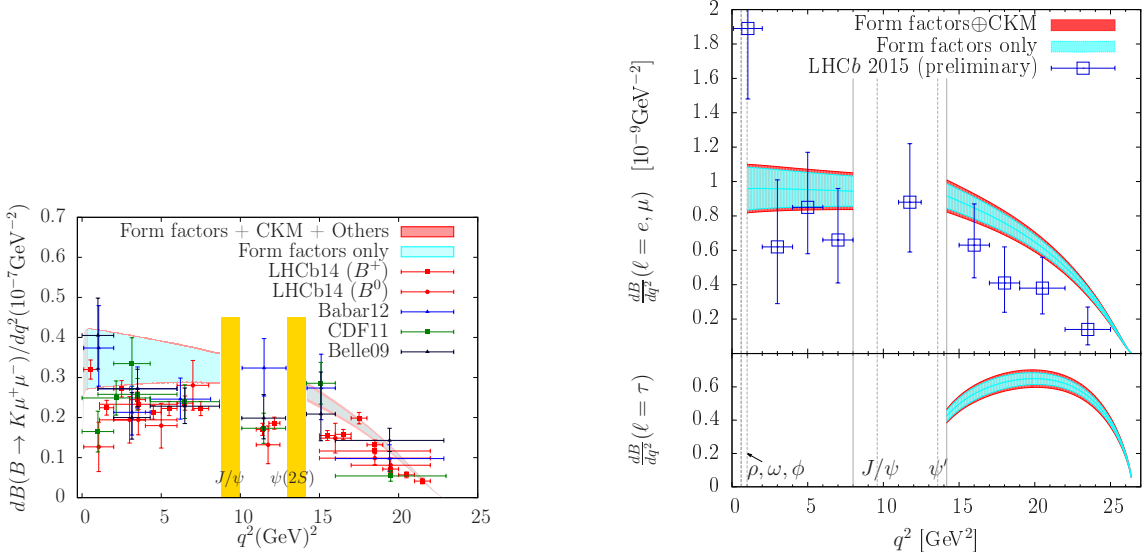


**Figure 7:** Left: A comparison of a recent standard-model lattice calculation of the differential branching fraction for  $B^+ \rightarrow K^+ \mu^+ \mu^-$  with experimental measurements [40, 41, 42, 46]. The lattice values are from an improved analysis [43] of form factor results from [44]. The Belle, CDF, and BaBar experiments report isospin averages. Right: A similar comparison for the observable  $B^+ \rightarrow \pi^+ \mu^+ \mu^-$ . The lattice result is from [47] and the experimental measurement is from LHCb [48].

in Fig. 7 with recent experimental measurements. For both processes the lattice values tend to lie slightly above the experimental points. The combined tension with the standard model is  $1.7\sigma$  [43].

## 2.7 Direct CP violation in $K$ decays

Calculating the amplitudes for the purely hadronic weak decay  $K \rightarrow \pi\pi$  has been a decades-long challenge for lattice gauge theory. In the past year the RBC-UKQCD collaboration announced the first controlled lattice calculation with physical kinematics that accounts numerically for the famous  $\Delta I = 1/2$  rule – namely, that the amplitude for the isospin zero ( $I = 0$ ) final state is considerably larger than that of the  $I = 2$  final state [49]. The calculation also yielded a value for the direct



**Table 1:** Comparison of results from the RBC-UKQCD collaboration [49] and from Ishizuka *et al.* [50] with experimental values [51] for the  $I = 0$  and  $I = 2$  amplitudes for the decay  $K \rightarrow \pi\pi$  and for the direct CP-violating ratio  $\epsilon'/\epsilon$ . The RBC-UKQCD calculation is done with physical kinematics. Errors in the Ishizuka *et al.* values are statistical only.

	RBC-UKQCD	Ishizuka <i>et al.</i>	experiment
$\text{Re}(A_0) \times 10^8$ (GeV)	46.6(10.0) <sub>stat</sub> (12.1) <sub>sys</sub>	24.26(38)	33.201(18)
$\text{Re}(A_2) \times 10^8$ (GeV)	1.50(4) <sub>stat</sub> (14) <sub>sys</sub>	60(36)	1.474(4)
$\text{Re}(\epsilon'/\epsilon) \times 10^4$	1.38(5.15) <sub>stat</sub> (4.43) <sub>sys</sub>	0.8(3.5)	16.6(2.3)

CP-violating ratio  $\epsilon'/\epsilon$ . The calculation was done with domain-wall fermions. The new results are listed in Table 1 and compared with recent results from Ishizuka *et al.* [50] and experimental values. The RBC-UKQCD result for  $\text{Re}(\epsilon'/\epsilon)$  is  $2.1\sigma$  below the experimental value.

## 2.8 Quark-flavor-physics conclusions

A wealth of new data from KEK-*B* and the LHC plus high-precision lattice-QCD calculations are producing ever more stringent tests of the standard model. The tension between inclusive and exclusive determinations of  $|V_{cb}|$  and  $|V_{ub}|$  remains. New searches for physics beyond the standard model appeared this year. There is some tantalizing tension in rare  $B$  decays, but still no unambiguous signs of new physics. We look forward to Belle-II, BES-III, and the LHC Run 2. In the meantime, the lattice-QCD community must work hard to keep up with experiment!

## 3. Spectroscopy highlights

Given the limitations of time, I will concentrate on calculations in the charmonium sector where there has been good recent progress. I will first discuss how the lattice methodology has evolved. For a more extensive review, see Ref. [52].

The time-honored method for determining the hadron spectrum works with the correlator of a pair of hadron interpolating operators with suitable quantum numbers, for example, the fermion bilinear  $\mathcal{O} = \bar{q}\gamma_\mu q$ . The correlation function between pairs selected from a set of such operators,

$$C_{ij}(t) = \langle 0 | \mathcal{O}_i(t) \mathcal{O}_j(0) | 0 \rangle, \quad (3.1)$$

is a matrix. In terms of the eigenenergies  $E_n$  of the hamiltonian, it takes the multiexponential form

$$C_{ij}(t) = \sum_n Z_{in} \exp(-E_n t) Z_{nj}. \quad (3.2)$$

Since the lattice has a finite volume, the spectrum  $E_n$  is always discrete. At sufficiently large time  $t$  the rhs is dominated by the lowest energy states. Those are the most reliably determined energies. For recent charmonium examples, see Refs. [53, 54].

The problem of extracting the eigenenergies can be reformulated as a variational calculation. The interpolating operators act on the vacuum to produce a variational basis set  $\mathcal{O}_i|0\rangle$ . That set then evolves in Euclidean time. As with any variational calculation, success in determining the



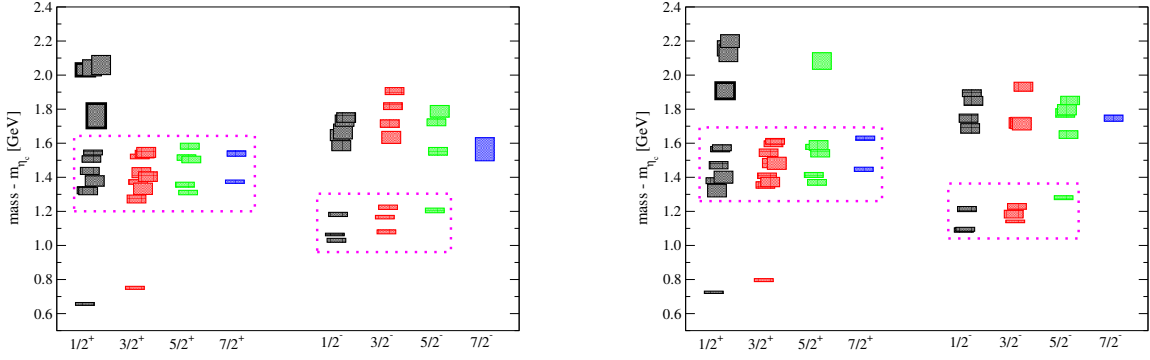


**Figure 8:** Spectrum of charm  $C = 2$  baryons (left panel,  $\Xi_{cc}'$ ; right panel,  $\Omega_{cc}$ ) from a recent calculation by the Hadron Spectrum Collaboration [55].

eigenenergies depends on how well the evolved variational basis set overlaps with the eigenstates themselves. So if the basis set consists of only quark bilinears, we might worry that we would have trouble describing states with a large open-charm component, such as  $D\bar{D}$ . Thus calculations with only quark bilinears have done well describing charmonium levels below the open charm threshold, but become increasingly unreliable at higher energies. For an example of an impressive calculation of this type for charmonium with many proposed excited and exotic charmonium states, see Ref. [56]. In the past year the same methods have been applied to charm  $C = 2$  baryons as shown in Fig. 8.

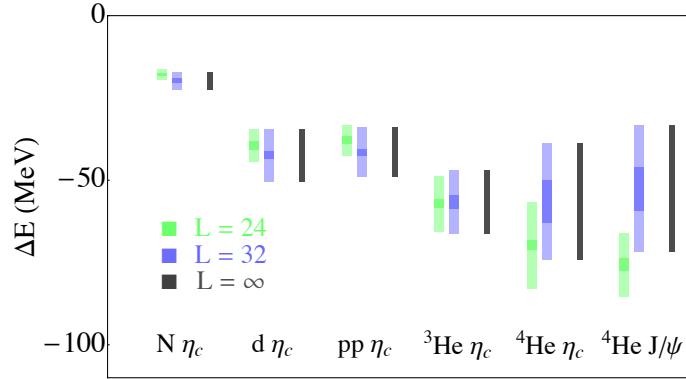


**Figure 9:** Binding energies for charmonium with light nuclei from Ref. [58], shown for two box sizes and an infinite volume extrapolation. Caution: the calculation was done at the  $SU(3)$ -flavor-symmetric point, so with  $M_\pi \approx 805$  MeV.

Particularly to study states that couple strongly to nearby multihadronic states, we must incorporate multihadronic states explicitly in the analysis. For identifying weakly bound states, a the more conventional nonvariational analysis suffices. An interesting recent example, particularly in light of increasing evidence for pentaquark states involving charm quarks [57] is a study of the binding of charmonium to nuclei by the NPLQCD collaboration [58]. Here one starts with an interpolating operator that creates both the charmonium state and the nucleus in question and measures the difference between the ground state energy of the combined, interacting system and the total energy of the noninteracting component hadrons. Some results are shown in Fig. 9 and suggest

binding energies of the order of several tens of MeV for light nuclei.

For charmonium, in the past few years attention has shifted to the study of excited levels using the variational method with two types of interpolating operators: quark bilinears and multi-quark operators that create explicit open charm state, such as  $D\bar{D}$ . Then it becomes possible to study resonant and other states whose existence is strongly influenced by nearby open charm levels. For states below inelastic threshold a method developed by Lüscher leads to the scattering phase shift. In the case of a resonance one then determines not only the resonant energy but also the width. In the case of a shallow bound state, one can also determine the binding energy. n

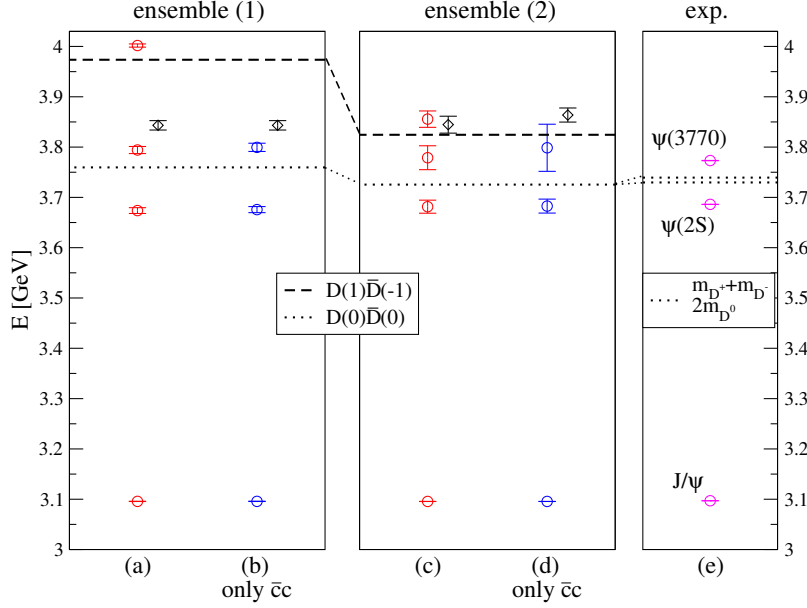


**Figure 10:** Finite box energies for the charmonium  $T_1^{--}$  channel containing both  $1^{--}$  and  $3^{--}$  states from Ref. [63]. Two different box sizes are used (left:  $L = 1.98$  fm, middle:  $L = 2.90$  fm). Dashed lines show noninteracting energies of two discrete  $D(p)\bar{D}(-p)$  scattering states with  $p = 2\pi/L$  and  $4\pi/L$ . Red points come from a full variational basis including both  $\bar{c}c$  and  $D(p)\bar{D}(-p)$  state. Blue points come from a reduced basis restricted to  $\bar{c}c$ . Black diamonds indicate a  $3^{--}$  assignment.

The Lüscher method exploits the physics of interacting hadrons confined to a finite box [59]. In a finite box the spectrum is discrete and depends on the linear box dimension  $L$ . If one can assume that the interaction takes place over a distance  $R$  less than  $L/2$  then the discrete box energies carry information about the infinite-volume elastic scattering amplitude — hence the infinite-volume elastic phase shift. In the simplest case of two identical particles of mass  $M$ , one uses

$$E_n = 2\sqrt{p_n^2 + M^2} \quad (3.3)$$

to convert a given discrete box energy level  $E_n$  into an “interacting momentum”  $p_n$ . The Lüscher analysis then leads to an infinite-volume phase shift  $\delta_n$  at that momentum  $p_n$ . These values can be interpolated to obtain  $\delta(p)$ . At a different value  $L$  one can obtain a new set of values for the same function  $\delta(p)$  to improve the interpolation. In the  $S$  wave, the infinite-volume elastic scattering amplitude is, as usual,

$$T(p) = \frac{1}{p \cot \delta(p) - ip}. \quad (3.4)$$

Poles correspond to bound states or resonances. The method can be generalized to the inelastic (coupled-channel) case [60, 61, 62].

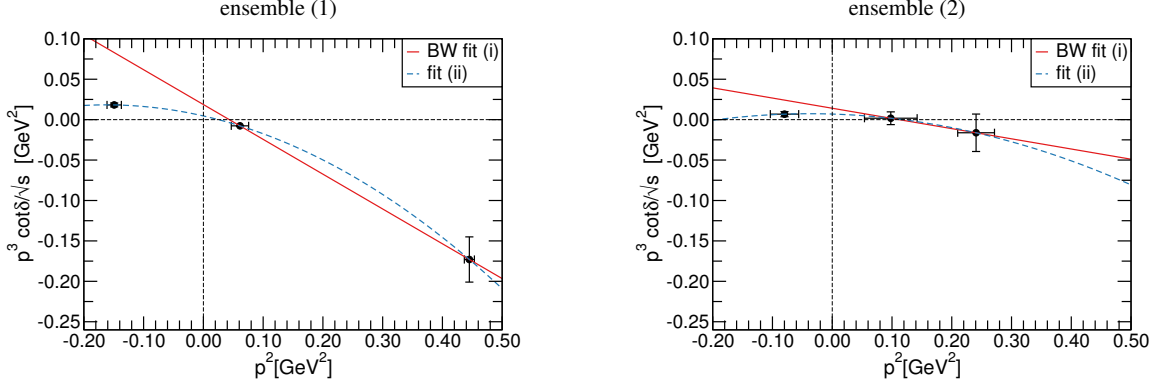


**Figure 11:** Phase shifts resulting from the finite-box states in Fig. 10 from Ref. [63].

When used in conjunction with multiple interpolating operators, the Lüscher method becomes a powerful tool for studying excited charmonium states. For a recent example, we point to work by Lang, Lescovac, Mohler, and Prelovsek [63] who looked at the charmonium state  $\psi(3770)$ , a  $J^{PC} = 1^{--}$   $P$ -wave resonance just above the  $D\bar{D}$  threshold. Figure 10 shows their discrete box energies for two different box sizes and different sets of interpolating operators. The resulting phase shifts are plotted in Fig. 11. The zero in  $p \cot \delta(p)$  just above  $DD$  threshold is identified as the  $\psi(3770)$ .

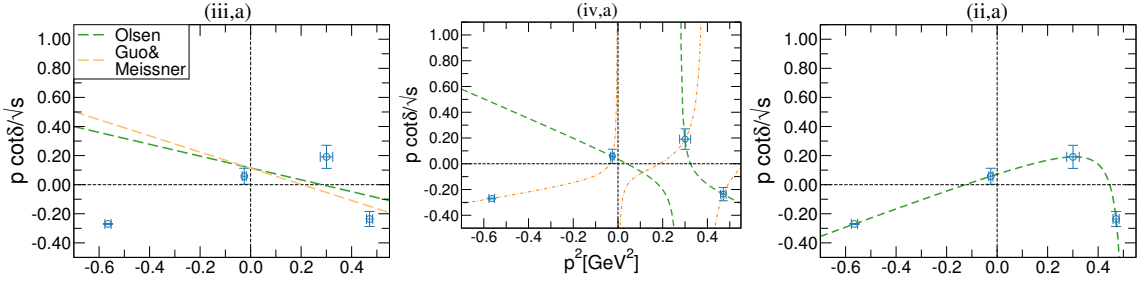


**Figure 12:** Results of fitting the lattice scalar  $D\bar{D}$  phase shift to a variety of parameterizations in a study of the  $X(3915)$  [63]. Left (rejected): one broad Breit-Wigner resonance, middle (rejected): two Breit-Wigner resonances, right (preferred): one narrow resonance and the  $\chi_{c0}(1P)$  state.

In the same project, Lang, Lescovac, Mohler, and Prelovsek also looked at the  $X(3915)$ , judged by the PDG to be a narrow scalar enhancement above threshold, perhaps the charmonium  $\chi_{c0}(2P)$  state. Lang *et al.* extract the phase shift and try a variety of parameterizations. Results for various hypotheses are shown in Fig. 12. Their preferred parameterization is consistent with the well-known  $1P$  bound state plus a narrow resonance around approximately 4 GeV. However, Zhou, Xiao, and Zhou make a case that the correct  $J^{PC}$  assignment for the state is  $2^{++}$  [64], so this story is still unfinished.

The  $1^{++}$  charmonium state  $X(3872)$  has been the subject of study in lattice QCD for the past few years. It is remarkably close to (less than 1 MeV below) the  $D\bar{D}^*$  threshold. It is therefore expected to be strongly influenced by the open charm threshold. The quark model predicts a  $\chi_{c1}(2P)$

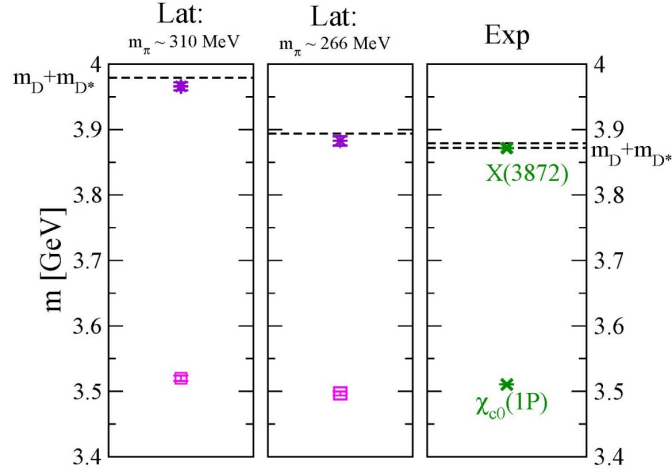


**Figure 13:** Comparison of results for the spectrum in the charmonium  $1^{++}$  channel from two lattice calculations. Left: Ref. [66], middle: Ref. [65] and right: experimentally measured masses. Dashed lines indicate the  $D\bar{D}^*$  threshold. The  $X(3872)$  candidate is just below it. (Figure credit: [52].)

state in the vicinity. For these reasons the theoretical understanding of the state should take into account both  $\bar{c}c$  states and open charm state. Results for the spectrum from calculations by Lescovic and Prelovsek [65] and later calculations by Lee *et al.* [66] are shown in Fig. 13. These calculations are done with different lattice ensembles, different light valence quarks at unphysical masses and at only one lattice spacing. However, both see an  $X(3872)$  candidate as a shallow bound state of  $D\bar{D}^*$ . Both use the Lüscher method, but some phenomenological arguments suggest that the state is quite large (perhaps 6 fm) [67], larger than the lattice box size, so it is important to test the result for finite volume effects.

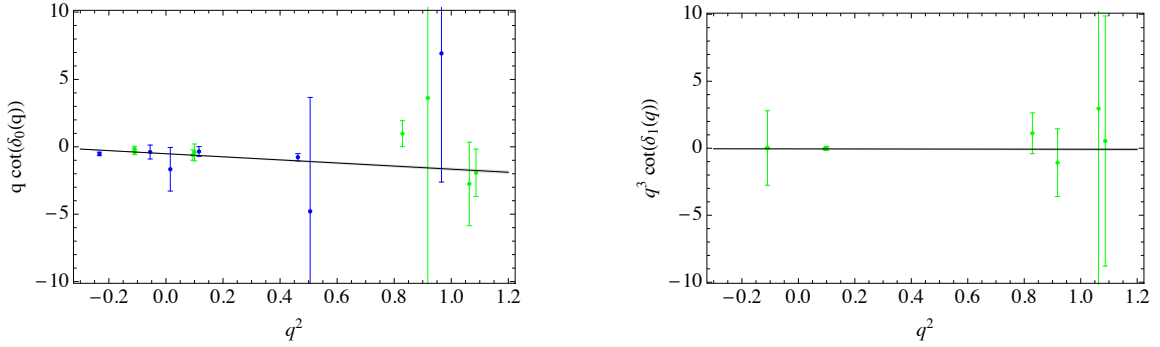


**Figure 14:** The  $S$ -wave and  $P$ -wave phase shifts for  $D\bar{D}^*$  scattering from a recent lattice QCD study by the CLQCD collaboration [68]. There is no sign of a resonance in either channel.

Unlike the  $X(3872)$ , the  $Z_c(3900)$  has not been found in lattice QCD studies so far [68]. The result of a recent effort is shown in Fig. 14. No  $S$ - or  $P$ -wave resonance was found.

### 3.1 Spectroscopy conclusions

New spectroscopic methods combine a multichannel analysis with Lüscher's formalism. There

has been rapid progress in understanding charmonium resonances and bound states close to an elastic threshold. The  $X(3872)$  could be a shallow  $D\bar{D}^*$  bound state but more work is needed to check finite size effects. The  $X(3915)$  needs more study. The  $Z_c(3900)$  has thus far escaped detection in a lattice study.

**Acknowledgments** I am grateful to Andreas Kronfeld, Daniel Mohler, and Ruth Van de Water for assistance with these proceedings. This work is supported by the U.S. National Science Foundation under grant PHY10-034278.

## References

- [1] S. Borsanyi *et al.* [BMW], Science **347**, 1452 (2015) [[arXiv:1406.4088](#) [hep-lat]].
- [2] S. Aoki *et al.* [FLAG], Eur. Phys. J. C **74**, 2890 (2014) [[arXiv:1310.8555](#) [hep-lat]].
- [3] A. Ukawa, talk, this conference (2015).
- [4] C. M. Bouchard, PoS (LATTICE2014) 002 (2015) [[arXiv:1501.03204](#) [hep-lat]].
- [5] R. Van de Water, CIPANP 2015, Vail, Colorado, May 20, 2015, <http://indico.wlab.yale.edu/indico/event/2/session/7/contribution/358>.
- [6] Carlos Peña, plenary talk, Lattice 2015 <http://indico2.riken.jp/indico/getFile.py/access?contribId=353&>.
- [7] R. Van de Water, European Physical Society Conference on High Energy Physics, Vienna, July 27, 2015, <https://indico.cern.ch/event/356420/session/19/contribution/13>.
- [8] J. L. Rosner, S. Stone and R. S. Van de Water, [arXiv:1509.02220](#) [hep-ph].
- [9] A. X. El-Khadra, A. S. Kronfeld and P. B. Mackenzie, Phys. Rev. D **55**, 3933 (1997) [[hep-lat/9604004](#)].
- [10] N. H. Christ, M. Li and H. W. Lin, Phys. Rev. D **76**, 074505 (2007) [[hep-lat/0608006](#)].
- [11] G. P. Lepage, L. Magnea, C. Nakhleh, U. Magnea and K. Hornbostel, Phys. Rev. D **46**, 4052 (1992) [[hep-lat/9205007](#)].
- [12] J. M. Flynn, T. Izubuchi, T. Kawanai, C. Lehner, A. Soni, R. S. Van de Water and O. Witzel [RBC/UKQCD], Phys. Rev. D **91**, 074510 (2015) [[arXiv:1501.05373](#) [hep-lat]].
- [13] J. A. Bailey *et al.* [Fermilab Lattice and MILC], Phys. Rev. D **92**, 014024 (2015) [[arXiv:1503.07839](#) [hep-lat]].
- [14] P. del Amo Sanchez *et al.* [BaBar], Phys. Rev. D **83**, 032007 (2011) [[arXiv:1005.3288](#) [hep-ex]].
- [15] J. P. Lees *et al.* [BaBar], Phys. Rev. D **86**, 092004 (2012) [[arXiv:1208.1253](#) [hep-ex]].
- [16] H. Ha *et al.* [Belle], Phys. Rev. D **83**, 071101 (2011) [[arXiv:1012.0090](#) [hep-ex]].
- [17] A. Sibidanov *et al.* [Belle Collaboration], Phys. Rev. D **88**, no. 3, 032005 (2013) [[arXiv:1306.2781](#) [hep-ex]].
- [18] J. A. Bailey *et al.* [MILC], Phys. Rev. D **92**, 034506 (2015) [[arXiv:1503.07237](#) [hep-lat]].
- [19] H. Na *et al.* [HPQCD], Phys. Rev. D **92**, 054510 (2015) [[arXiv:1505.03925](#) [hep-lat]].

- [20] B. Aubert *et al.* [BaBar], Phys. Rev. D **79**, 012002 (2009) [[arXiv:0809.0828 \[hep-ex\]](#)].
- [21] R. Glattauer, European Physical Society Conference on High Energy Physics, Vienna, July 27, 2015. <https://indico.cern.ch/event/356420/session/3/contribution/306>.
- [22] P. Gambino, European Physical Society Conference on High Energy Physics, Vienna, July 27, 2015. <https://indico.cern.ch/event/356420/session/3/contribution/824>.
- [23] J. P. Lees *et al.* [BaBar], Phys. Rev. Lett. **109**, 101802 (2012) [[arXiv:1205.5442 \[hep-ex\]](#)].
- [24] J. F. Kamenik and F. Mescia, Phys. Rev. D **78**, 014003 (2008) [[arXiv:0802.3790 \[hep-ph\]](#)].
- [25] J. A. Bailey *et al.*, Phys. Rev. Lett. **109**, 071802 (2012) [[arXiv:1206.4992 \[hep-ph\]](#)].
- [26] M. Huschle *et al.* [Belle], Phys. Rev. D **92**, 072014 (2015) [[arXiv:1507.03233 \[hep-ex\]](#)].
- [27] R. Aaij *et al.* [LHCb], Phys. Rev. Lett. **115**, 111803 (2015) [Phys. Rev. Lett. **115**, 159901 (2015)] [[arXiv:1506.08614 \[hep-ex\]](#)].
- [28] Y. Amhis *et al.* [HFAG], [arXiv:1412.7515 \[hep-ex\]](#). With online update [http://www.slac.stanford.edu/xorg/hfag/semi/eps15/eps15\\_dtanu.html](http://www.slac.stanford.edu/xorg/hfag/semi/eps15/eps15_dtanu.html).
- [29] J. A. Bailey *et al.* [Fermilab Lattice and MILC], Phys. Rev. D **89**, 114504 (2014) [[arXiv:1403.0635 \[hep-lat\]](#)].
- [30] W. Detmold, C. Lehner and S. Meinel, Phys. Rev. D **92**, 034503 (2015) [[arXiv:1503.01421 \[hep-lat\]](#)].
- [31] A. Alberti, P. Gambino, K. J. Healey and S. Nandi, Phys. Rev. Lett. **114**, 061802 (2015) [[arXiv:1411.6560 \[hep-ph\]](#)].
- [32] A.S. Kronfeld, private communication (2015).
- [33] A. Bazavov *et al.*, Phys. Rev. D **86**, 034503 (2012) [[arXiv:1205.7013 \[hep-lat\]](#)].
- [34] C. Albertus *et al.*, Phys. Rev. D **82**, 014505 (2010) [[arXiv:1001.2023 \[hep-lat\]](#)].
- [35] E. Gamiz *et al.* [HPQCD], Phys. Rev. D **80**, 014503 (2009) [[arXiv:0902.1815 \[hep-lat\]](#)].
- [36] N. Carrasco *et al.* [ETM], JHEP **1403**, 016 (2014) [[arXiv:1308.1851 \[hep-lat\]](#)].
- [37] Y. Aoki, T. Ishikawa, T. Izubuchi, C. Lehner and A. Soni, Phys. Rev. D **91**, 114505 (2015) [[arXiv:1406.6192 \[hep-lat\]](#)].
- [38] J. Simone *et al.* [Fermilab Lattice and MILC], PoS (LATTICE2015) 332 (2015); <http://indico2.riken.jp/indico/contributionDisplay.py?contribId=277&sessionId=14&confId=1805>.
- [39] J. Laiho, E. Lunghi and R. S. Van de Water, Phys. Rev. D **81**, 034503 (2010) [[arXiv:0910.2928 \[hep-ph\]](#)]; update from E. Lunghi, private communication (2015).
- [40] J.-T. Wei *et al.* [Belle], Phys. Rev. Lett. **103**, 171801 (2009) [[arXiv:0904.0770 \[hep-ex\]](#)].
- [41] T. Aaltonen *et al.* [CDF], Phys. Rev. Lett. **107**, 201802 (2011) [[arXiv:1107.3753 \[hep-ex\]](#)].
- [42] J. P. Lees *et al.* [BaBar], Phys. Rev. D **86**, 032012 (2012) [[arXiv:1204.3933 \[hep-ex\]](#)].
- [43] D. Du, A. X. El-Khadra, S. Gottlieb, A. S. Kronfeld, J. Laiho, E. Lunghi, R. S. Van de Water and R. Zhou, [[arXiv:1510.02349 \[hep-ph\]](#)].
- [44] J. A. Bailey *et al.*, [arXiv:1509.06235 \[hep-lat\]](#).

- [45] C. Bouchard *et al.* [HPQCD], Phys. Rev. Lett. **111**, 162002 (2013) [Phys. Rev. Lett. **112**, 149902 (2014)] [[arXiv:1306.0434](#) [hep-ph]].
- [46] R. Aaij *et al.* [LHCb], JHEP **1406**, 133 (2014) [[arXiv:1403.8044](#) [hep-ex]].
- [47] J. A. Bailey *et al.* [Fermilab Lattice and MILC], Phys. Rev. Lett. **115**, 152002 (2015) [[arXiv:1507.01618](#) [hep-ph]].
- [48] R. Aaij *et al.* [LHCb], JHEP **1510**, 034 (2015) [[arXiv:1509.00414](#) [hep-ex]].
- [49] Z. Bai *et al.*, [[arXiv:1505.07863](#) [hep-lat]].
- [50] N. Ishizuka, K.-I. Ishikawa, A. Ukawa and T. Yoshië, Phys. Rev. D **92**, 074503 (2015) [[arXiv:1505.05289](#) [hep-lat]].
- [51] Particle Data Group, “CP Violation in  $K_L$  Decays”,  
<http://pdg.lbl.gov/2015/reviews/rpp2014-rev-cp-viol-kl-decays.pdf>.
- [52] S. Prelovsek, [arXiv:1508.07322](#) [hep-lat].
- [53] B. A. Galloway, P. Knecht, J. Koponen, C. T. H. Davies and G. P. Lepage, PoS(LATTICE2014)092 (2014) [[arXiv:1411.1318](#) [hep-lat]].
- [54] P. Pérez-Rubio, S. Collins and G. S. Bali, Phys. Rev. D **92**, 034504 (2015) [[arXiv:1503.08440](#) [hep-lat]].
- [55] M. Padmanath, R. G. Edwards, N. Mathur and M. Peardon, Phys. Rev. D **91**, 094502 (2015) [[arXiv:1502.01845](#) [hep-lat]].
- [56] L. Liu *et al.* [Hadron Spectrum], JHEP **1207**, 126 (2012) [[arXiv:1204.5425](#) [hep-ph]].
- [57] R. Aaij *et al.* [LHCb], Phys. Rev. Lett. **115**, 072001 (2015) [[arXiv:1507.03414](#) [hep-ex]].
- [58] S. R. Beane, E. Chang, S. D. Cohen, W. Detmold, H.-W. Lin, K. Orginos, A. Parreño and M. J. Savage [NPLQCD], Phys. Rev. D **91**, 114503 (2015) [[arXiv:1410.7069](#) [hep-lat]].
- [59] M. Lüscher, Nucl. Phys. B **364**, 237 (1991).
- [60] M. T. Hansen and S. R. Sharpe, Phys. Rev. D **86**, 016007 (2012) [[arXiv:1204.0826](#) [hep-lat]].
- [61] R. A. Briceno and Z. Davoudi, Phys. Rev. D **88**, 094507 (2013) [[arXiv:1204.1110](#) [hep-lat]].
- [62] P. Guo, J. Dudek, R. Edwards and A. P. Szczepaniak, Phys. Rev. D **88**, 014501 (2013) [[arXiv:1211.0929](#) [hep-lat]].
- [63] C. B. Lang, L. Leskovec, D. Mohler and S. Prelovsek, JHEP **1509**, 089 (2015) [[arXiv:1503.05363](#) [hep-lat]].
- [64] Z. Y. Zhou, Z. Xiao and H. Q. Zhou, Phys. Rev. Lett. **115**, 022001 (2015) [[arXiv:1501.00879](#) [hep-ph]].
- [65] S. Prelovsek and L. Leskovec, Phys. Rev. Lett. **111**, 192001 (2013) [[arXiv:1307.5172](#) [hep-lat]].
- [66] S. H. Lee *et al.* [Fermilab Lattice and MILC], [[arXiv:1411.1389](#) [hep-lat]].
- [67] E. Braaten, PoS(EFT09)065 (2009).
- [68] Y. Chen *et al.*, Phys. Rev. D **89**, 094506 (2014) [[arXiv:1403.1318](#) [hep-lat]].